State-resolved UV photofragmentation spectrum of the metal dication complex $[Zn(pyridine)_4]^{2+}$

Guohua Wu,[a] Caroline Norris,[b] Hamish Stewart,[a] Hazel Cox*[b] and Anthony J. Stace*[a]

Received (in Cambridge, UK) 16th April 2008, Accepted 21st May 2008
First published as an Advance Article on the web 11th July 2008
DOI: 10.1039/b806469e

A combined theoretical and experimental study of electronic transitions in the complex $[Zn(pyridine)_4]^{2+}$ provides the first example of a state-resolved electronic spectrum to be recorded for a dication complex in the gas phase.

The UV-visible spectra of metal complexes are routinely recorded in the condensed phase either in solution or in the form of a matrix.[1] As a consequence of the high density, discrete transitions between the electronic states of a complex are frequently obscured by inhomogeneous broadening. Although cooling can improve resolution, differences in site symmetry still influence results. In addition, condensed phase spectra are recorded in the presence of a counterion, which in itself can have a contributing spectrum and, if highly charged, can perturb the spectrum and structure of the ion of interest. In contrast, measurements of spectra in the gas phase can be performed both on isolated species and in the absence of a counterion,[2] and for singly charged ions vibrational state resolution has been achieved.[3,4] However, many of the metal ion complexes that have been studied in this way are not representative of ions in their more common oxidation states.

The development of new techniques for the generation and study of stable multiply charged metal complexes in the gas phase has seen considerable progress in recent years,[5–10] and it is now possible to access a wide range of metals and charge states. However, further progress in the field requires spectroscopic experiments that are capable of yielding structural information on the ions; either directly in terms of geometry, or in terms of an electronic configuration that can be related to geometry. Since multiply charged ions cannot generally be cooled by the usual technique of adiabatic expansion,[11] alternative procedures need to be developed in order to simplify spectra. Reported here are the first results from an experiment in which it has been possible to cool a multiply charged ion in order to resolve individual electronic transitions that contribute to a UV photofragmentation spectrum. The results presented are for the metal dication complex $[Zn(pyridine)_4]^{2+}$, where calculations show that electronic transitions can be assigned to within 550 cm^{-1}.

Neutral zinc–pyridine clusters were prepared using the pick-up technique, and the ion of interest was generated from these by high energy electron impact ionisation.[12] Mass-selected $[Zn(pyridine)_4]^{2+}$ complexes were fed into a Paul ion trap, in which the end caps were continuously cooled by contact with a liquid nitrogen reservoir and where, over a total trapping period of 1 s, collisions with a helium buffer gas (5×10^{-4} mbar) led to a considerable reduction in the internal energy content of the ions.[13] Although difficult to estimate, the temperature of the ions was thought to be somewhere in the range 100–150 K; this contrasts with the $\sim +400$ K internal temperature the ions have when they emerge from the ionisation stage of the experiment. This estimate is based on the observation that the latter ions exhibit unimolecular decay.[12] Calculated binding energies for several of the complexes studied in earlier spectroscopic experiments were found to be higher than the energy received from a single photon,[6] therefore photofragmentation at visible wavelengths relied on the ions being 'hot' for the appearance of fragments. Since high binding energies are also expected to be the case here,[14] the centre of attention of the experiments has shifted to UV wavelengths in order to ensure that photofragmentation is a one-photon process.

Following cooling, the ions were irradiated with pulsed (7 ns), tunable UV radiation taken as the frequency-doubled output from a Nd:YAG-pumped dye laser. Absorption of a photon led to the loss of a single neutral pyridine molecule, and the intensities of both precursor and fragment ions were monitored as a function of photon energy, with the latter changing in steps of 5 cm^{-1}. Ions that had been accumulated and cooled within the trap for 300 ms, were irradiated with 7 laser pulses before being ejected for mass analysis and signal averaging. This cycle was repeated 200 times to yield a photofragment mass spectrum, and a typical example recorded at 40 180 cm^{-1} is shown in Fig. 1, where the precursor and fragment ions can clearly be seen. The ion $[Zn(pyridine)_3H_2O]^{2+}$ is also present, where the co-ordinately unsaturated Zn(II) photofragment has attracted a water molecule from the background. Cooling helped to minimise this problem; however, when it occurred, the $[Zn(pyridine)_3H_2O]^{2+}$ ion intensity was added to the fragment signal.

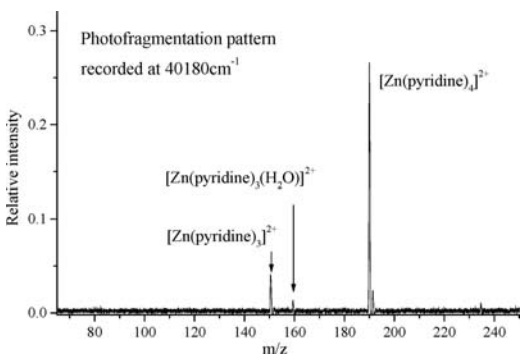

Fig. 1 Example of a photofragmentation mass spectrum recorded at a photon energy of 40 180 cm^{-1}. The assignment of ions is discussed in the text.

[a] *Department of Physical Chemistry, School of Chemistry, The University of Nottingham, University Park, Nottingham, UK NG7 2RD. E-mail: tony.stace@nottingham.ac.uk*
[b] *Department of Chemistry and Biochemistry, University of Sussex, Falmer, Brighton, UK BN1 9QJ. E-mail: H.Cox@Sussex.ac.uk*

Calculations on the structure and electronic excitation energies of the $[Zn(pyridine)_4]^{2+}$ complex were performed using the Amsterdam density functional program (ADF).[15–18] The calculations were performed at the all electron level with a Slater-type orbital basis set of triple zeta plus two polarisation functions (TZ2P) and with default convergence criteria. Geometry optimisations were performed using the local density approximation (LDA) due to Vosko *et al.*[19] The lowest energy structure was found to have D_{2d} symmetry. Excitation energies and oscillator strengths were calculated using time dependent density functional theory (TDDFT).[20–23] The LDA functional was used in the SCF step, and the standard adiabatic local density approximation (ALDA)[24] in the post SCF step. LDA is valid for these calculations as the energy of the LDA calculated HOMO is −13.20 eV, and well below the spectral range considered here.[25] To help in the interpretation of excitation spectra, calculations were also performed on the pyridine molecule at the same level of theory.

Fig. 2 shows a plot of photofragment yield as a function of photon energy together with the electronic transitions and oscillator strengths predicted for $[Zn(pyridine)_4]^{2+}$. The calculations show there are no dipole-allowed transitions below 37 000 cm^{-1}. The experimental data have been normalised with respect to precursor ion intensity and laser power.

Initial experiments just covered the spectral range 37 000–40 500 cm^{-1} and recorded the three features seen within that band. It was unclear at that stage as to whether the features were the result of multiple electronic excitations or of a single electronic excitation, which was coupled to an excited vibrational mode. Gaseous pyridine is known to exhibit vibrational structure on transitions to low-lying excited states (see for example ref. 26 and 27), and this is accompanied by geometric distortion.[28,29] Previous TDDFT calculations on $[Ag(pyridine)_4]^{2+}$,[7] showed that there were relatively few electronic excitations contained within a broad absorption band recorded at visible wavelengths.

In a D_{2d} $[Zn(pyridine)_4]^{2+}$ complex there are 129 normal modes of vibration, of which 18 lying between 30–3132 cm^{-1} have A_1 symmetry and are thus capable of coupling with dipole-allowed electronic transitions. Four low lying modes involve the Zn–pyridine bond and the remaining A_1 modes involve pyridine vibrations that can be assigned using the classification of Innes *et al.*,[30] based on that of Wilson for benzene.[31] There are 4 A_1 modes lying within 100 cm^{-1} of the experimental peak separations of ~960 cm^{-1}. They are at 946, 1001, 1040 and 1042 cm^{-1}. The first two are both classified as type "Ho", out-of-plane CH bends, the third is of "Cp" type, an in-plane ring bend, and the fourth is of "CC" type, a carbon–carbon stretch.[30] Of the four modes considered, the latter would be most likely to preserve the "allowedness" of the first electronic transition (a ^1E which is a $\pi^* \leftarrow \pi$ transition). If it couples to this excitation at 38 020 cm^{-1} this would give rise to peaks at 39 062 and 40 104 cm^{-1} which is in very good agreement with the dominant peaks at 39 220 and 40 141 cm^{-1}. The increase in intensity seen between 37 000 and 40 500 cm^{-1} could then be rationalised in terms of better Franck–Condon overlap with the distorted excited state. However it does not account for the secondary peak at 38 427 cm^{-1}, and provides no explanation of why only this one vibration is excited.

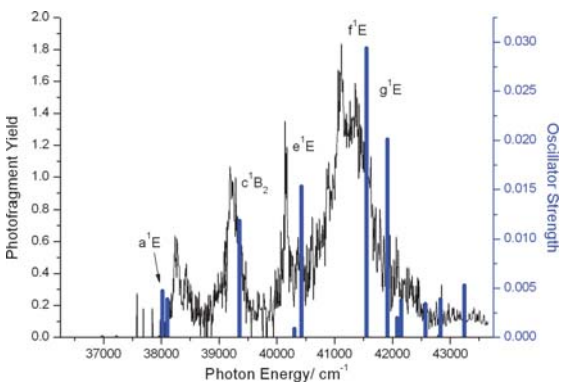

Fig. 2 Photofragmentation yield plotted as a function of photon energy. The vertical lines are calculated electronic excitation energies and their heights are proportional to the calculated oscillator strengths. All allowed excitations are shown and the dominant transitions are assigned (TDDFT).

In contrast, the initial photofragmentation features did align extremely well with calculated transitions between electronic states. The first transition to have a significant oscillator strength (~0.005) at 38 020 cm^{-1}, lies within 250 cm^{-1} of an experimental feature, and other, higher energy excitations are also a good match with experimental peaks, and the calculated oscillator strengths match the photofragmentation yield of the main features extremely well. In addition, a strong transition (oscillator strength 0.0294) was predicted to appear just outside the preliminary experimental range at ~41 500 cm^{-1}, and further experiments confirmed this to be the case.

Table 1 summarises the observed spectral features and their calculated assignments in terms of dipole-allowed electronic transitions. Also given are the oscillator strengths and the molecular and/or complex orbitals involved. For at least eight of the calculated transitions (including all the dominant transitions highlighted in bold) there are peaks in the experimental spectrum that are within 550 cm^{-1} of the predicted excitation energies. For other calculated transitions there are also experimental peaks within this range, however the assignments are less certain (shown in brackets).

The transitions appear to fall into three categories: (i) $f \geq 0.01$ and can be closely matched to experimental features purely in terms of dominance, and with excellent, quantitative agreement between theory and experiment; (ii) $0.01 > f \geq 0.003$ and these excitations are assigned purely on position and relative (rather than absolute) magnitude, but again there is good agreement; (iii) $f < 0.003$ and these transitions are not observed experimentally. These data give a good indication of oscillator strengths (or more precisely, orders of relative magnitude) required when predicting future spectra of multiply-charged metal ligand complexes.

The first two excitations in Table 1 correspond to $\pi^* \leftarrow \pi$ transitions; these are purely ligand based, and involve all four pyridine molecules in each molecular orbital of the complex. A comparison with isolated pyridine shows that these excitations are to the $^1B_2$ state, which, depending on experimental technique, is reported to lie at 38 360 cm^{-1}[30] or 40 274 cm^{-1}.[32] The presence of the Zn^{2+} ion/additional pyridine molecules induces a red-shift relative to that seen in the isolated molecule.

The next 3 significant transitions are from a combined metal–ligand orbital to π^* molecular orbitals that are purely ligand based. The ground-state orbital includes contributions from all four nitrogen lone pairs together with a small amount of metal

Table 1 Summary of observed and TDDFT electronic transitions[32] and oscillator strengths, *f*. Dominant transitions are shown in bold

Peak position/cm^{-1}					
Observed	Calculated	*f*	Assignment[b]		
38 254	38 020	0.0047	LLCT	$\pi^* \leftarrow \pi$	a ^{1}E
38 427	38 105	0.0039	LLCT	$\pi^* \leftarrow \pi$	b ^{1}B$_2$
39 220	**39 350**	**0.0119**	**MLLCT**	$\boldsymbol{\pi^* \leftarrow \sigma}$	c ^{1}**B$_2$**
—	40 303[a]	0.0009	MLLCT	$\pi^* \leftarrow \sigma$	d ^{1}E
40 141	**40 425**	**0.0153**	**MLLCT**	$\boldsymbol{\pi^* \leftarrow \sigma}$	e ^{1}**E**
41 123	**41 548**	**0.0294**	**MLLCT**	$\boldsymbol{\pi^* \leftarrow \sigma}$	f ^{1}**E**
41 363	**41 911**	**0.0201**	**LLCT**	$\boldsymbol{\pi^* \leftarrow \pi}$	g ^{1}**E**
—	42 082[a]	0.0020	LLCT	$\pi^* \leftarrow \pi$	h ^{1}B$_2$
(41 786)	42 151	0.0038	MLLCT	$\pi^* \leftarrow \sigma$	i ^{1}B$_2$
(42 067)	42 575	0.0034	LLCT	$\pi^* \leftarrow \pi$	j ^{1}E
—	42 805[a]	0.0001	MLLCT	$\pi^* \leftarrow \sigma$	k ^{1}E
42 435	42 831	0.0039	LLCT	$\pi^* \leftarrow \pi$	l ^{1}B$_2$
42 850	43 247	0.0053	LLCT	$\pi^* \leftarrow \pi$	m ^{1}E

[a] Photofragmentation but no discernable peak. [b] MLLCT: metal/ligand to ligand charge transfer; LLCT: ligand to ligand charge transfer.

character (5–9%). These transitions are best described as metal/ligand to ligand CT (MLLCT), and are assigned as $\pi^* \leftarrow \sigma$, despite their derivation from the $^1B_1$ $\pi^* \leftarrow n$ transition in the isolated pyridine molecule. The latter appears at 34 771 cm^{-1}[30] or 35 835 cm^{-1},[33] and is the first allowed singlet transition in pyridine. The effect of the dication/additional pyridines is to blue-shift the excitations by over 4000 cm^{-1} relative to that recorded for an isolated pyridine molecule. The most intense observed excitation in the spectrum is in the MLLCT category. The second strongest transition at ~41 400 cm^{-1} (41 911 cm^{-1} calculated) is assigned as $\pi^* \leftarrow \pi$ and is derived from a $^1A_1$ excitation in the isolated pyridine molecule. In the latter, this excitation appears at 49 800 cm^{-1}[30] or 49 498 cm^{-1},[33] meaning that it is red-shifted by the presence of the metal dication/additional pyridine ligands.

A result of particular interest is the experimental feature seen at ~41 100 cm^{-1}, where the ground state involves an orbital of the complex that is calculated to include a small contribution from an atomic orbital on Zn^{2+}. Closed-shell metal cations, such Zn^{2+}, Mg^{2+}, and Ca^{2+}, lack spectroscopic signatures at accessible visible and UV wavelengths. Therefore, there is a continual search for electronic transitions in receptor molecules that are influenced by the presence of such an ion.[34] In many instances, suitable receptors coordinate Zn^{2+} through interactions with nitrogen atoms that are either part of, or attached to, an aromatic framework.[35–37]

In this work, TDDFT has produced surprisingly accurate results that successfully guided the experiment to locate the dominant peak at 41 100 cm^{-1}. However, the quality of the experimental spectra reported here sets demanding new tests for theory. Given the level of agreement between theory and experiment, one would assume that the excitation of such a complex is essentially adiabatic and the spectrum is electronic, however, a vibrational progression can not be completely dismissed. Therefore, to truly understand the fine structure (and be confident that a single-reference calculation is adequate), methods capable of optimising excited state geometries (and including multi-reference character) appear to be an important next step. From these experiments on Zn^{2+}, and other closed shell metal dications that do not have characteristic electronic transition at UV-visible wavelengths, accurate assignments of spectra will make an important contribution to the development of markers for detecting their presence in an environmental or biological context.

The authors would like to thank the EPSRC for financial support and for the award of studentships to CN and HS. HC and CN would like to thank the EPSRC National Service for Computational Chemistry Software (NSCCS) (url: http://www.nsccs.ac.uk) for computer time and Prof. Tony McCaffery for helpful discussions.

Notes and references

1 A. B. P. Lever, *Inorganic Electronic Spectroscopy*, Elsevier, Amsterdam, 1984.
2 M. A. Duncan, *Annu. Rev. Phys. Chem.*, 1997, **48**, 69.
3 T. D. Vaden and J. M. Lisy, *J. Phys. Chem. A*, 2005, **109**, 3880.
4 E. D. Pillai, T. D. Jaeger and M. A. Duncan, *J. Phys. Chem. A*, 2005, **109**, 3521.
5 L. Pŭskar and A. J. Stace, *J. Chem. Phys.*, 2001, **114**, 6499.
6 L. Pŭskar, H. Cox, A. Goren, G. D. C. Aitken and A. J. Stace, *Faraday Discuss.*, 2003, **124**, 259.
7 J. Guan, L. Pŭskar, R. O. Esplugas, H. Cox and A. J. Stace, *J. Chem. Phys.*, 2007, **127**, 064311.
8 T. G. Spence, B. T. Trotter, T. D. Burns and L. A. Posey, *J. Phys. Chem. A*, 1998, **102**, 6101.
9 C. J. Thompson, J. Husband, F. Aguirre and R. B. Metz, *J. Phys. Chem. A*, 2000, **104**, 8155.
10 A. J. Stace, *J. Phys. Chem. A*, 2002, **106**, 7993.
11 N. R. Walker, G. A. Grieves, J. B. Jaeger, R. S. Walters and M. A. Duncan, *Int. J. Mass Spectrom.*, 2003, **228**, 285.
12 B. J. Duncombe, L. Pŭskar, B. Wu and A. J. Stace, *Can. J. Chem.*, 2005, **83**, 1994.
13 G. Wu, D. Chapman and A. J. Stace, *Int. J. Mass Spectrom.*, 2007, **262**, 211.
14 The dissociation energy calculated for the loss of pyridine from $[Zn(pyridine)_4]^{2+}$ is 2.39 eV: C. Norris and H. Cox, unpublished results.
15 *ADF*, SCM, Theoretical Chemistry, Vrije Universiteit, Amsterdam, The Netherlands, 2007, http://www.scm.com.
16 C. Fonseca Guerra, J. G. Snijders, G. te Velde and E. J. Baerends, *Theor. Chem. Acc.*, 1998, **99**, 391.
17 E. J. Baerends and B. te Velde, *J. Comput. Phys.*, 1992, **99**, 84.
18 G. te Velde, F. M. Bickelhaupt, E. J. Baerends, C. F. Guerra, S. A. van Gisbergen, J. G. Snijders and T. Ziegler, *J. Comput. Chem.*, 2001, **22**, 931.
19 S. H. Vosko, L. Wilk and M. Nusair, *Can. J. Phys.*, 1980, **58**, 1200.
20 S. J. A. van Gisbergen, J. G. Snijders and E. J. Baerends, *Comput. Phys. Commun.*, 1999, **118**, 119.
21 F. Wang and T. Ziegler, *Mol. Phys.*, 2004, **102**, 2585.
22 F. Wang and T. Ziegler, *J. Chem. Phys.*, 2004, **121**, 12191.
23 F. Wang and T. Ziegler, *J. Chem. Phys.*, 2005, **122**, 074109.
24 E. K. U. Gross and W. Kohn, *Adv. Quantum Chem.*, 1990, **21**, 255.
25 M. E. Casida, C. Jamorski, K. C. Casida and D. R. Salahub, *J. Chem. Phys.*, 1998, **108**, 4439.
26 U. Ölsher, R. Lubart and M. Brith, *Chem. Phys.*, 1976, **17**, 237.
27 A. Bolovinos, P. Tsekeris, J. Philis, E. Pantos and G. Andritsopoulos, *J. Mol. Spectrosc.*, 1984, **103**, 240.
28 S. I. Nagaoka and U. Nagashima, *J. Phys. Chem.*, 1990, **94**, 4467.
29 Z. M. Su, Y. H. Kan, Z. H. Huang, Y. Liao, Y. Q. Qui and R. S. Wan, *Synth. Met.*, 2003, **137**, 1095.
30 K. K. Innes, I. G. Ross and W. R. Moomaw, *J. Mol. Spectrosc.*, 1988, **132**, 492.
31 E. B. Wilson, Jr, *Phys. Rev.*, 1934, **45**, 706.
32 All dipole-allowed excitations calculated between 0–43 000 cm^{-1} are included in Table 1 except for two weak transitions with $f < 10^{-5}$.
33 I. C. Walker, M. H. Palmer and A. Hopkirk, *Chem. Phys.*, 1989, **141**, 365.
34 S. C. Burdette and S. J. Lippard, *Inorg. Chem.*, 2002, **41**, 6816.
35 H. Chen, Y. Wu, Y. Cheng, H. Yang, F. Li, P. Yang and C. Huang, *Inorg. Chem. Commun.*, 2007, **10**, 1413.
36 A. E. Dennis and R. C. Smith, *Chem. Commun.*, 2007, 4641.
37 W. Jiang, Q. Fu, H. Fan and W. Wang, *Chem. Commun.*, 2008, 259.